Generation of tumors in wing imaginal discs of *Drosophila melanogaster* third instar larvae to study temporal and spatial patterns of expression of major heat shock proteins

Gunjan Singh and Subhash C. Lakhotia*

Cytogenetics Laboratory, Department of Zoology, Banaras Hindu University, Varanasi, 221005, India

* Corresponding author

Email:

Gunjan Singh: gunjan.mhg.bhu10@gmail.com

S. C. Lakhotia: lakhotia@bhu.ac.in

ORCID ID:

Gunjan Singh: **0000-0002-4458-180X**

S. C. Lakhotia: **0000-0003-1842-8411**

Running Title: Heat shock proteins in age-defined *Drosophila* tumors

Key words: MARCM somatic clones; lgl, activated Ras, Yorkie, Hsp, F-actin

Abstract

Cancer cells experience a variety of stresses like hypoxia, lack of nutrients, DNA damage and immune responses, which trigger several processes to drive genomic instability and mutation, alterations in gene expression programs, and reprogramming of the metabolic pathways to escape growth inhibition signaling, and acquire resistance to the immune surveillance. Different heat shock proteins are expressed at elevated levels in cancer cells. However, their specific roles in initiation, establishment and progression of cancers are still not clear. Here using the loss of function allele of the apico-basal polarity gene, *lgl*, we have established models for induction of tumorous somatic clones of different genetic constitutions at defined developmental times for examination of temporal and spatial patterns of expression of the major heat shock protein families, namely Hsp83, Hsp70, Hsp60 and Hsp27. The Hsp83, Hsp60 and Hsp27 begin to express in all cells of the tumor at high levels since early stages (48hr after tumor induction) and continue their high expression at later stages when the tumorous clones accumulate F-actin and get transformed. Levels of the heat shock cognate Hsc70 proteins also follow the same pattern as the other Hsps. However, the major stress-inducible Hsp70 is not expressed at early stages of tumor growth, but expresses at a later stage only in a few cells in a given *lgl* loss of function clone, which also shows high F-actin aggregates. Thus, the major Hsps, except the Hsp70, seems to be involved in early as well as late stages of epithelial tumors induced by loss of the Lgl cell polarity protein, while the Hsp70 expression in a few cells coincides with their getting transformed. This model will be useful for further genetic studies to dissect specific roles of different Hsps in tumor development and their therapeutic manipulation.

Introduction

Drosophila has remained a very good model for studying various aspects of carcinogenesis. Homologs of nearly 50 mammalian tumor suppressor genes were identified and molecularly characterized in *Drosophila* during the past century and recent genome wide screens, typically employing a combination of knockdown and/or mis-expression of genes have been used to create tumors of the desired type, have identified many more genes in *Drosophila* that are associated with tumorigenesis in mammalian system as well (Ugur et al 2016; Mirzoyan et al 2019; Kanda and Igaki 2020). This has been facilitated by development of new models for studying cooperative tumorigenesis in distinct developing larval tissues as these serve as responsive fields for specific genetic manipulations to modulate activities of well-known growth regulators. Imaginal discs, the undifferentiated epithelial bag like structures within the larval body, metamorphose into specific 3-dimensional appendages of the adult through cellular proliferation and pattern formation during the pupal period (Fristrom et al 1970; Fristrom and Fristrom, 1975). Each disc is a two layered epithelial structure, with flat and wide squamous peripodial epithelial cells on one side while tall and thin columnar epithelium comprises the disc proper. The internally facing side of the squamous and columnar epithelial cells correspond to their apical surfaces (Drubin and Nelson, 1996). The basolateral domains of these cells communicate with neighboring cells and the extra-cellular matrix via cell surface receptors and other membrane proteins, and the components responsible for generating cell surface asymmetry are evolutionarily conserved cell polarity proteins, whose loss of function leads either to hyperplasia or to neoplastic transformation (Hutterer et al 2004; Román-Fernández and Bryant 2016; Mechler et al 1985; Agarwal et al 1995).

One of the most commonly studied *Drosophila* tumor suppressor gene is the *lethal* (*2*) *giant larvae* (*lgl*), which encodes the p127 or Lgl protein. Lgl establishes the apical-basal polarity by regulating the delivery of vesicles to specific domains in plasma membrane (Parsons et al 2014) and plays crucial role in regulating asymmetric cell divisions (Betschinger et al 2003). Loss of the p127 protein in *lgl* loss of function mutants leads to malignant cancer because of the loss of epithelial organization, excessive proliferation and invasive behavior of the imaginal disc and brain cells in the developing third instar larva (Gateff and Schneiderman, 1974; Froldi et al 2008).

Cancer cells face a range of stressful conditions like hypoxia, lack of nutrients, DNA damage and immune responses (Hanahan and Weinberg 2011; Calderwood and Murshid 2017; Lang

et al 2019). Therefore, cancer cells trigger several processes to drive genomic instability and mutation, alterations in gene expression programs, and reprogramming of the metabolic pathways to escape growth inhibition signaling, and acquire resistance to the immune surveillance. Therefore, understanding the cross talk between different stress response pathways provides better therapeutic approaches. Different Hsps are expressed at increased levels in cancer cells (Calderwood et al 2006; Calderwood and Gong 2016; Calderwood and Murshid 2017; Lang et al 2019). However, their specific roles in initiation, establishment and progression of cancers are still not clear.

In order to examine these issues, we have used a strategy to generate tumorous wing discs or somatic clones of tumorous cells in wing discs in *Drosophila* larvae for a systematic temporal mapping of expression of Hsps during tumor growth. We primarily utilized lgl^{-} *(l(2)*gl^{4}) null mutant allele induced tumors in larval wing discs. Loss of *lgl* function was accomplished by either down regulating its transcripts through RNAi with the *MS1096* or *Act5c-GAL4* driver or by inducing *FLP-FRT* mediated *lgl* mutant somatic clones in lgl^{+}/lgl^{-} background using the MARCM technique (Lee and Luo 1999; Lee and Luo 2001). Since the *lgl* mutant somatic clones by themselves do not grow well (Agrawal et al 1995; Menéndez et al 2010), tumor co-operators like Yorkie or activated Ras or Pvr were co-overexpressed in lgl^{-} clones. Following the standardization of the experimental set up, the spatial patterns of expression of the major Hsps, viz., Hsp83, Hsp70, Hsp60 and Hsp27 at specified time points after induction of tumors were examined.

Materials & Methods

Fly strains: Fly stocks and experimental crosses were reared on standard agar-maize powder-sugar food at 24±1^{0}C. The following fly stocks were used to set up crosses to obtain progeny of desired type: 1. *w; lgl*^{4} *FRT40A/CyO; Sb/TM6B*; 2.*y w hsFLP; FRT40A* w^{+} y^{+}*/CyO-GFP*; 3. *Y w hsFLP tubGAL4 UAS-GFP; tubGAL80 FRT40A/CyO-GFP; +/+ (MARCM* stock); 4.*w; lgl*^{4} *FRT40A UAS-yki /CyO-GFP; +/+*; 5. *w; lgl*^{4} *FRT40A UAS-Ras*^{v12} */CyO-GF; 6.* w^{1118}*; UAS-Ras*^{V12}*/CyO; +/+* (BDSC-4847); 7. *MS1096-Gal4; +/+; +/+* (Capdevila and Guerrero 1994); 8. *w; UAS-Ras*^{v12}*/CyO-GFP ; +/+*; 9. *w; +/+; lgl-RNAi*; 10. *w; UAS-yki /CyO-GFP* (*UAS-yki* referred to as *yki*^{OE} 11. w^{*}*; +/+; P{y[+t7.7] w[+mC]=UAS-yki.S111A.S168A.S250A.V5}attP2* (BDSC-28817); this transgene is referred to as *UAS-yki*$^{Act;}$ 12. *w; UAS-Ras*^{v12}*/CyO-GFP; lgl-RNAi; 13.w; UAS-yki/CyO-GFP; lgl-RNAi*.

The stocks 1-6 were obtained from Prof. Pradip Sinha (IIT Kanpur; see Khan et al 2016) while others were either available in our laboratory or were obtained from the Bloomington Drosophila Stock Centre (BDSC). Appropriate crosses were carried out as required.

Generation of tumors in wing imaginal discs

With a view to generate epithelial tumors in larval wing imaginal discs, *l(2)gl*^{4} mutation (referred to here as *lgl*$^{-}$) or *lgl-RNAi* has been primarily used to disrupt cell polarity. In addition, transgenes like *UAS-Ras*^{v12}, and *UAS-yki,* that conditionally disrupt cell polarity when driven by an appropriate GAL4 driver, were also used. Two strategies were used for tumor induction: i) *MS1096-GAL4* driven expression of *UAS* carrying transgene in the wing pouch region (Capdevila and Guerrero 1994), and ii) the MARCM (**M**osaic **A**nalysis with a **R**epressible **C**ell **M**arker) technique (Lee and Luo 1999; Lee and Luo 2001) approach, which allows generation of *lgl*$^{-}$ homozygous cell clones in *lgl*$^{-}$/+ genetic background.

Males of the desired genotype were crossed with *MS1096-GAL4* females. Synchronized 1st instar progeny larvae were collected during a 2-hour larval hatching window at 24±1°C. and grown at 24±1°C till late third instar stage. Samples of tumorous wing discs were collected by dissecting the desired progeny larvae at different time-points (counted as "days After Egg laying", "d AEL"), which varied from 5d AEL to 7d AEL.

In the 2nd approach involving generation of somatic clones in wing discs, MARCM technique (Lee and Luo, 1999) was employed using males of the desired genotype for crossing with MARCM genotype females. The progeny larvae were heat shocked (see below) to activate *hs-FLP* for induction of clones that were homozygous either for *lgl*$^{-}$ or *lgl*$^{-}$ *UAS-yki* or *lgl*$^{-}$ *UAS-Ras*^{V12} mutation/transgene. For reasons not known, and not explored, reciprocal crosses did not generate clones. Synchronized 1st instar progeny larvae from the various crosses that hatched within a 2hour window were collected and reared at 24±1°C. Larvae of different ages were heat shocked at 37°C for different durations to induce FLP-mediated somatic recombination (see Results). The non-CyO-GFP larvae were selected and dissected at different time-points (counted as "days After Clone Induction" = "d ACI"), varying from 1 to 7d ACCI to study the growth dynamics of tumorous clones in wing imaginal discs of different genotypes.

Survival assay: In order to study the effect of tumorous clones on the survival of host, larvae carrying tumors were grown at 24°C till adult emergence. Numbers of those dying as early or pseudo-pupae and as late pupae (pharate) and of the emerging flies were counted.

Fluorochromes: Chromatin was visualized with staining with DAPI (4', 6-diamidino-2-phenylindole dichloride, Sigma-Aldrich, India**)** at 1µg/ml concentration. Filamentous action (F-actin) was stained with Phalloidin-Atto 633 **(**Sigma-Aldrich, India using 1:40 dilution).

Immunostaining: The following primary antibodies were used: 1. Anti-Hsp27 (Abcam-ab49919; 1:40 dilution) raised in mouse for detecting *Drosophila* Hsp27; 2. Anti-Hsp60 (CST-SP60, D307#4870; 1:50 dilution) raised in rabbit for detecting *Drosophila* Hsp60; 3. Anti-Hsp70 (7Fb, a kind gift by Dr. M. B. Evgenev; 1:200 dilution) raised in rat, which exclusively detects the stress inducible *Drosophila* Hsp70 (Velazquez and Lindquist, 1984); 4. Anti-Hsp/Hsc70 (3.701, Sigma-Aldrich, India; Velazquez and Lindquist, 1984) antibody raised in rat detects both inducible as well as constitutive forms, i.e., Hsp70 and Hsc70 proteins (Velazquez and Lindquist, 19845). Anti-Hsp83 (a kind gift by Dr. Robert Tanguay, 3E6; 1:50 dilution) raised in mouse, to detect Hsp83 of *Drosophila melanogaster* (Morcillo et al 1993). Appropriate Alexa Fluor (Molecular Probes, USA) or Cy3 (Sigma-Aldrich, India) tagged secondary antibodies were used at the manufacturer's recommended dilution to detect the primary antibody.

The wing imaginal discs were dissected out in Phosphate Buffered Saline (1X PBS: 130 mm NaCl, 7 mm Na_2HPO_4, 3mm KH_2PO_4, of pH 7.2) from larvae of the desired age and genotype and fixed with 3.5% paraformaldehyde in 1X PBS for 40 min and further processed for immunostaining as described earlier (Prasanth et al 2000). Immunostained discs were mounted in DABCO (1,4-diazabicyclooctane, Molecular Probes, UK) and examined under LSM510 Meta Zeiss laser scanning confocal microscope using appropriate laser, dichroic and barrier filters. Adobe Photoshop 7.0 was used to assemble all the images.

Results

Induction of somatic clones in wing imaginal discs:

In order to precisely define the time when a cell begins to develop as tumor, the MARCM (**M**osaic **A**nalysis for **R**epressible **C**ell **M**arker) technique was used to generate *lgl*$^-$ homozygous somatic clones at defined stage of larval development, with or without co-

expression of the other oncogenic proteins like Yki or Ras. Application of a pulse of heat shock at defined time in larval development point permitted specific studies on the temporal and spatial progression of the tumorous clones.

Among the larvae of different genotypes produced in MARCM crosses, those carrying the *lgl*$^-$ clones in imaginal discs were identified by absence of general GFP fluorescence (indicating absence of the *CyO-GFP* balancer chromosome) but presence of patches of GFP fluorescence in larval body due to the induced GFP expressing *lgl*$^-$ clones.

Standardization of Heat Shock (HS) treatment for induction of *lgl*$^-$ clones:

In order to standardize the duration of heat shock (HS) and age of larvae for induction of discrete somatic clones, virgin females from *y w hsFLP tubGAL4 UAS-GFP; tubGAL80 FRT40/ CyO-GFP* were crossed with *w; lgl*$^-$ *FRT40/CyO-GFP*; Sb/TM6B males in the first set of experiments. The progeny larvae of different ages (48hr, 72hr or 96hr AEL) were divided into 3 sets each. For each age, Set-1 larvae were exposed to 5min HS (37°C), Set-2 to 15min HS and Set-3 to 35min HS. Larvae from the different sets were screened to identify those carrying the MARCM clones. Wing discs of larvae of the desired genotype were dissected at 72hr ACI. Wing discs from larvae treated with different HS duration (Sets 1-3) at 48hr and 96hr AE, had only a few *lgl*$^-$ clones, while those from larvae exposed to HS at 72hr AEL generated discernible populations of *lgl*$^-$ clones (**Fig. 1**). Therefore, the 72hr AEL developmental stage was selected for determining the optimal duration of HS treatment for this genotype. Wing discs from Set-1 (5min HS at 72hr AEL) exhibited only a few clones (**Fig. 1a-a'**) with the adults emerging without any detectable deformities. Larvae from Set-2 (15min HS at 72hr AEL) showed good number of *lgl*$^-$ clones at 72hr ACI but most of them were eliminated at the later stages (96hr ACI, not shown) of tumor progression without affecting the cytoskeleton arrangement (**Fig. 1b, b'**). Larvae from Set-3 (35min HS at 72hr AEL) showed good numbers of clones at 72hr ACI, which got transformed by 96hr ACI as the tumor progressed (**Fig. 1c, c', e-e'''**). The emerging non-CyO (MARCM) adults were scored for deformities and necrotic patches in eyes, wings and thorax within 2-3 days of eclosion (Fig. **1f-i**). Duration of HS enhanced the frequency of adults with deformities. In order to see if heat shock to larvae by itself induced any developmental defects, y^+ w^+ *FRT40/ CyO-GFP* larvae, grown in parallel and similarly treated with HS as for inducing clones, were taken as control for comparing the adult deformities in flies emerging from heat shocked experimental non-CyO

(MARCM) adults. Adult flies emerging from these larvae did not show any abnormalities (**Fig. 1f, h, k**).

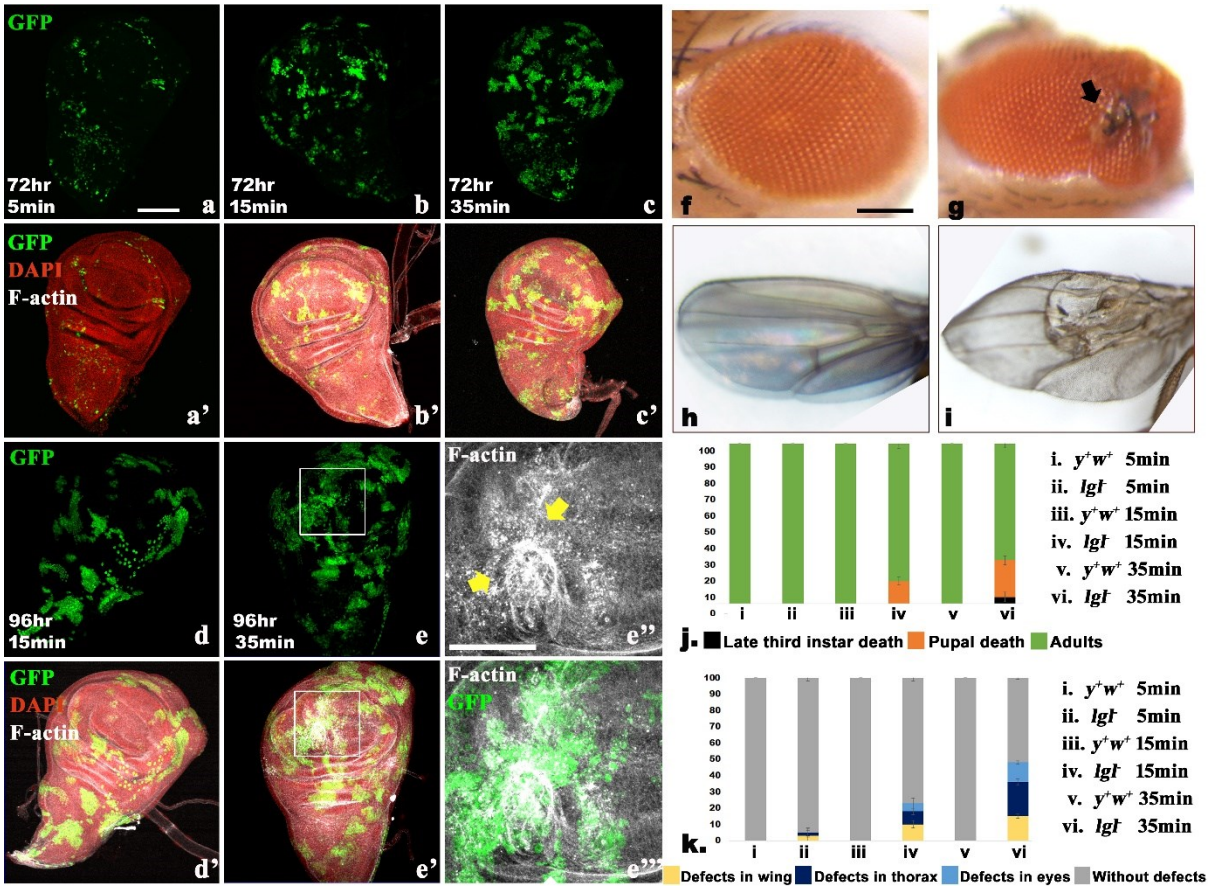

Fig. 1. Standardization of the duration of HS treatment for induction of *lgl⁻* somatic clones with *tubGAL4* driven GFP and their effect on the survival of the organism: Confocal optical sections of wing imaginal discs from third instar MARCM larvae heat shocked at 72hr AEL and examined at 72 or 96hr ACI showing GFP (green) positive *lgl⁻* somatic clones (**a-e'''**). The duration of HS is indicated at the lower left corner in **a-e**. Images in **a-e** show GFP (green) signal while those in **a'-e'** show GFP (green), DAPI (red) and F-actin (white) in the corresponding **a-e** discs, respectively. The marked areas in (**e-e'**) are presented at higher magnification in **e''** and **e'''**, respectively, to show the F-actin arrangement (white) in the GFP positive (green) clone. Yellow arrows indicate actin-nucleation. Scale bars in **a** and **e''** denote 50µm and applies to **a-e'** and **e'''**, respectively. **f-i:** images of adult eyes (**f-g**) and wings (**h-i**) in control, *y w hsFLP tubGAL4 UAS-GFP; y^+w^+FRT40/ CyO-GFP; +/+* (**f** and **h**) and *y w hsFLP tubGAL4 UAS-GFP; lgl^- FRT40/ CyO-GFP; +/+* (**g** and **i**) flies showing necrotic patch in eye (black arrow in **g**) and wing deformity (**h**). **j:** Histograms of mean percentages (± S.E.) of those dying as larvae or pupae and those emerging as adult flies (**Y-axis**) in different

genotypes (**X-axis**). **k:** Histograms of mean percentages (± S.E.) of deformities observed in adults (**Y-axis**) in response to varying durations of HS treatment in different genotypes (**i-vi** on **X-axis** with the abbreviated genotypes noted on the right side). The abbreviated genotypes in **j** and **k** correspond to**:** *y^+ w^+ = y w hsFLP tubGAL4 UAS-GFP; y^+w^+FRT40/ CyO-GFP; +/+* (control), and *lgl^- = y w hsFLP tubGAL4 UAS-GFP; lgl^- FRT40/ CyO-GFP; +/+* (MARCM clone carrying adults).

Standardization of Heat Shock (HS) treatment for selection of developmental stage and its duration to induce *lgl^- yki^{OE}* somatic clones and assessment of their effects on the survival of host:

Homozygosity for the loss-of-function mutants of *lgl (lgl^-)* generates neoplastic tumors in imaginal discs; however, such clones do not generally survive in *lgl^+/lgl^-* background due to their apoptosis caused by the cell-competition phenomenon (Agrawal et al 1995; Menendez et al 2010; Kanda and Igaki 2020). The *lgl^-* cells in *lgl^+* background can evade apoptosis if other oncogenic co-operators, which confer them proliferation advantage, are co-expressed (Menendez et al 2010; Daniel 2018). Co-expression of different oncogenic co-operators like *UAS-Ras^{v12}*or *UAS-yki* (*yki^{OE}*) or *UAS-yki^{Act}* promotes growth of the *lgl^-* cell clones. Overexpression of Yorkie*,* a component of Hippo pathway, positively regulates proliferation while inhibiting apoptosis (Huang et al 2005). Likewise, GAL4-driven expression of *UAS-Pvr^{Act}* transgene, which produces activated form of Platelet-derived Growth Factor and Vascular Endothelial Growth Factor-Receptor Related (Pvr), a homologue of VEGF pathway in *Drosophila*, also promotes survival of *lgl^-* cell clones (Heino et al 2001, Shibuya 2011).

In view of the different properties of growth of the *lgl^-* clones in the background of other oncogenic co-operator*s,* larval age and the duration of HS for inducing optimal mutant clones of these genetic backgrounds were re-examined. Virgin *y w hsFLP tubGAL4 UAS-GFP; tubGAL80 FRT40/ CyO-GFP* females were crossed with *w; lgl^- yki^{OE} FRT40 /CyO-GFP*; Sb/TM6B males and the progeny larvae were exposed to varying durations of HS and examined for the somatic clones generated in wing discs; survival of such larvae to adult stage was also monitored.

Since over-expression of Yorkie in *lgl^-* mutants provides uncontrolled neoplastic growth, it was necessary to re-identify the optimal larval stage when the HS would generate optimal numbers of *lgl^- yki^{OE}* somatic clones that can be followed for longer periods. The progeny larvae were

exposed to a 5min HS at different developmental stages and examined for the somatic clones generated in eye-antennal and wing discs at different time points ACI; the survival of such larvae to adult stage was also monitored. Compared to wild type, these larvae suffered a delay of approximately 24hr before they pupated.

HS was given at, 2nd instar (48hr AEL), early third instar (72he AEL) and middle (96hr AEL) third instar larvae respectively. 5min HS at 48hr AEL generated fused *lgl⁻ yki*^{OE} somatic clones when examined at 72hr ACI (**Fig. 2a, a'**). HS to larvae at 96hr AEL resulted in numerous clones, making it difficult to follow each clone distinctly at later stages of tumor progression (**Fig. 2c, c'**). HS treatment to early third instar larvae at 72hr AEL generated distinct clones in moderate numbers (**Fig. 2 b, b'**). HS at this time also provided a subsequent window of 72hr ACI to examine survival and growth of the induced *lgl⁻ yki*^{OE} somatic clones prior to their pupation (see the schematic in **Fig. 3**), which was not feasible when HS was given at 48hr AEL due to very small sized wing imaginal discs or at 96hr AEL which precluded study of 72hr old tumors as larvae pupated or died by then, see the schematic in **Fig. 3**). Similar results were obtained for induction of *lgl⁻ Ras*^{V12} somatic clones. Therefore, 72hr AEL was selected for the HS to generate the *lgl⁻ yki*^{OE} and *lgl⁻ Ras*^{V12} MARCM clones.

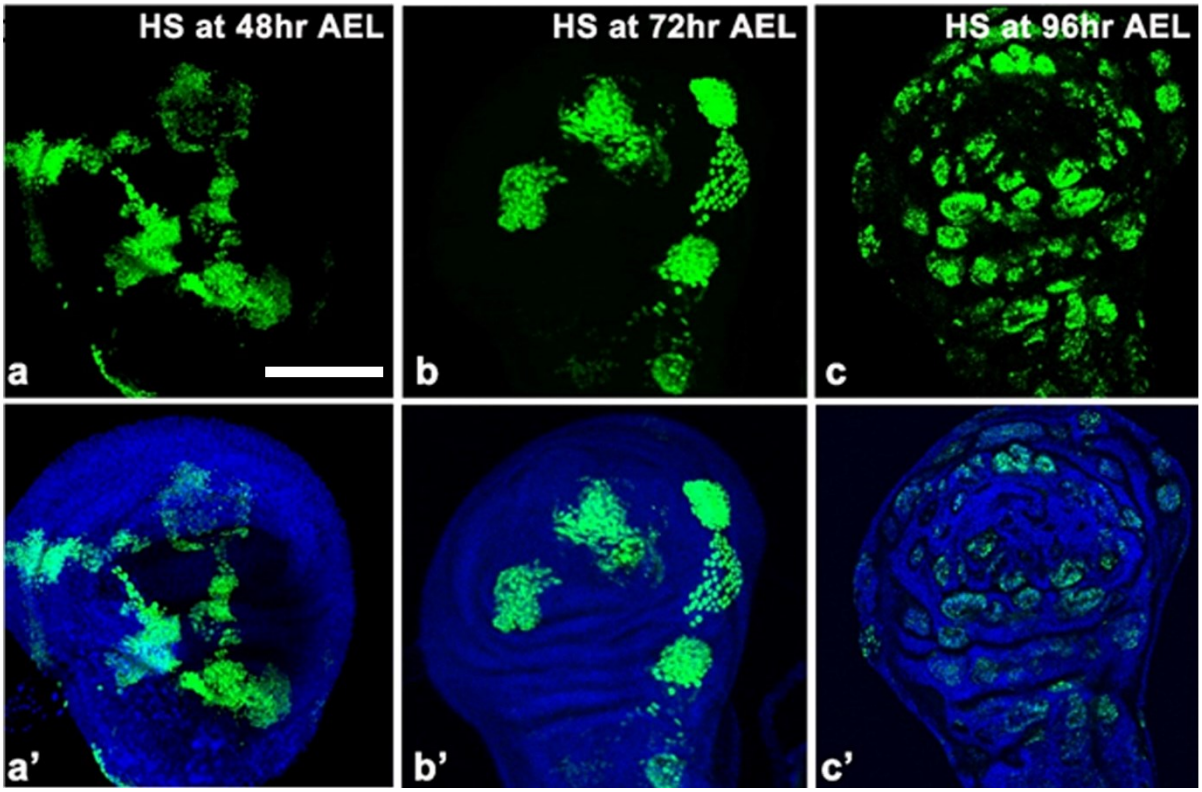

Fig. 2. HS treatment at different stages generated *lgl⁻ yki^OE* *MARCM* clones of different sizes when examined at 72hr ACI. 5min HS at 48hr AEL resulted in fused clones with GFP expressing (green) cells present all over the disc at 72hr ACI (**a, a'**). 5min HS at 72hr resulted in optimal numbers of GFP expressing discrete clones (green) at 48hr ACI, which could be examined for longer periods after HS (**b, b'**). 5min HS at 96hr AEL resulted in numerous GFP expressing (green) clones at 24hr ACI (**c, c'**). Images in **a'-c'** show combined GFP and DAPI fluorescence of discs shown in **a-c**, respectively. Scale bar in **a** denotes 50µm and applies to **a-c'**.

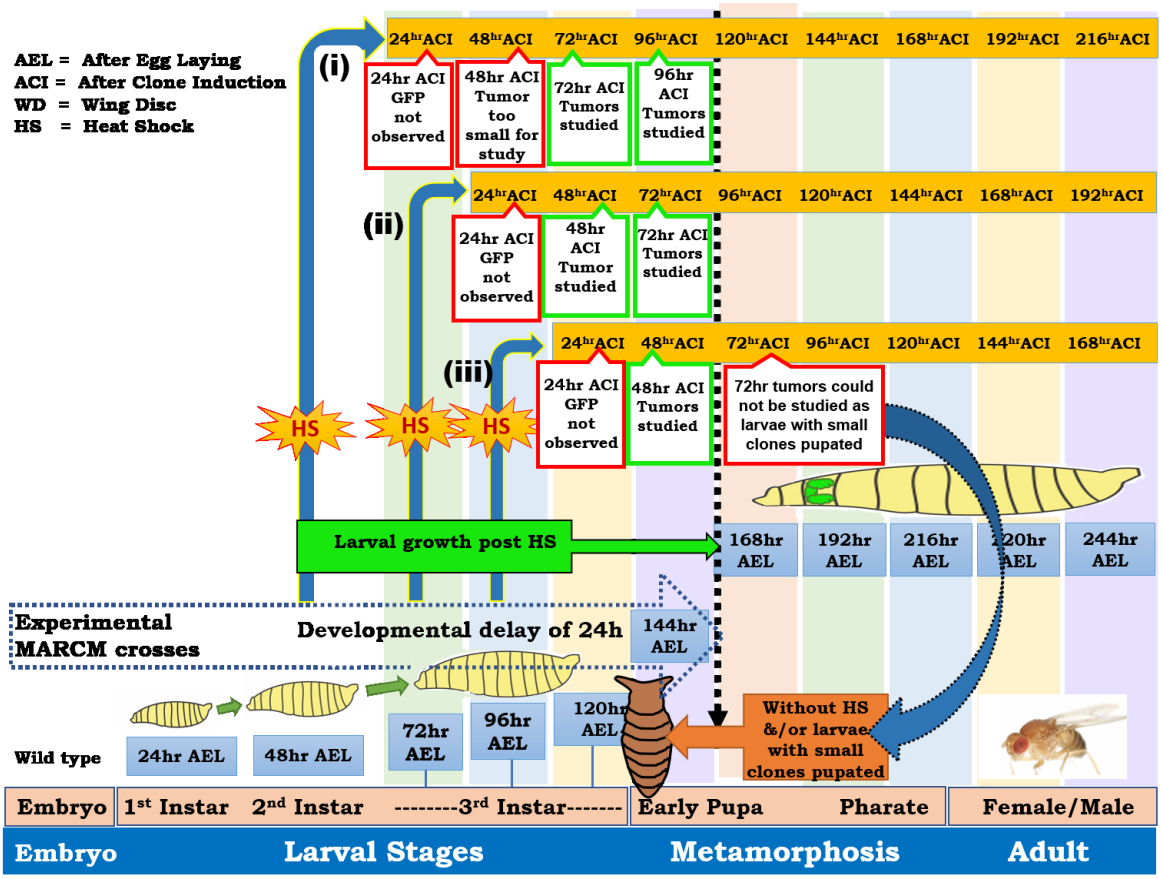

Fig. 3 Selection of developmental stage of larvae for the HS treatment for induction of *lgl⁻ yki^OE* clones using the *MARCM*: a schematic showing generation of clones following HS at different developmental stages and how it affected the analyzability of tumor progression. It is notable that the progeny larval from the *MARCM* crosses showed developmental delay of ~24hr before pupation.

In view of the more aggressive growth of *lgl⁻ yki^OE* or *lgl⁻ Ras^v12* clones, the duration of HS to 72hr larvae of this genotype was re-examined. Unlike in the *lgl⁻* clones (**Fig. 1**), HS treatment for 15min generated *lgl⁻ yki^OE* clones that overgrew and fused with each other at later stages of

tumor progression (**Fig. 4b-b', d- d', f-f'**) and thus affected tracking of individual clones. HS treatment for 2min (not shown) or 3min (**Fig. 4 a, a'. c-c', e-e'**) to 72hr old larvae induced fewer but discrete clones in wing imaginal discs which could be traced distinctly even up to 72 or 96hr ACI. Data on larval and pupal death following HS of different durations to 72hr old larvae to induce the *lgl⁻ yki*^{OE} clones are presented in **Fig. 4g**. As may be noted, HS for 5, 15 or 30min resulted in high larval and pupal lethality with very few surviving to adult stage. Approximately 50% of larvae exposed to 3min HS survived to adult stage (**Fig. 4 g**). Although the survival to adult stage was better when the 72hr larvae were heat shocked for 2min (**Fig. 4g**), it generated a lower frequency of clones. Therefore, the 3min HS treatment to 72hr old larvae was selected for subsequent studies because of better consistency in the number and sizes of induced *lgl⁻ yki*^{OE} somatic clones. However, the 3min HS could not generate similar numbers of *lgl⁻ Ras*^{v12} clones in, therefore such larvae were subjected to 5min HS treatment for generating somatic clones (**Fig. 4h-j'**).

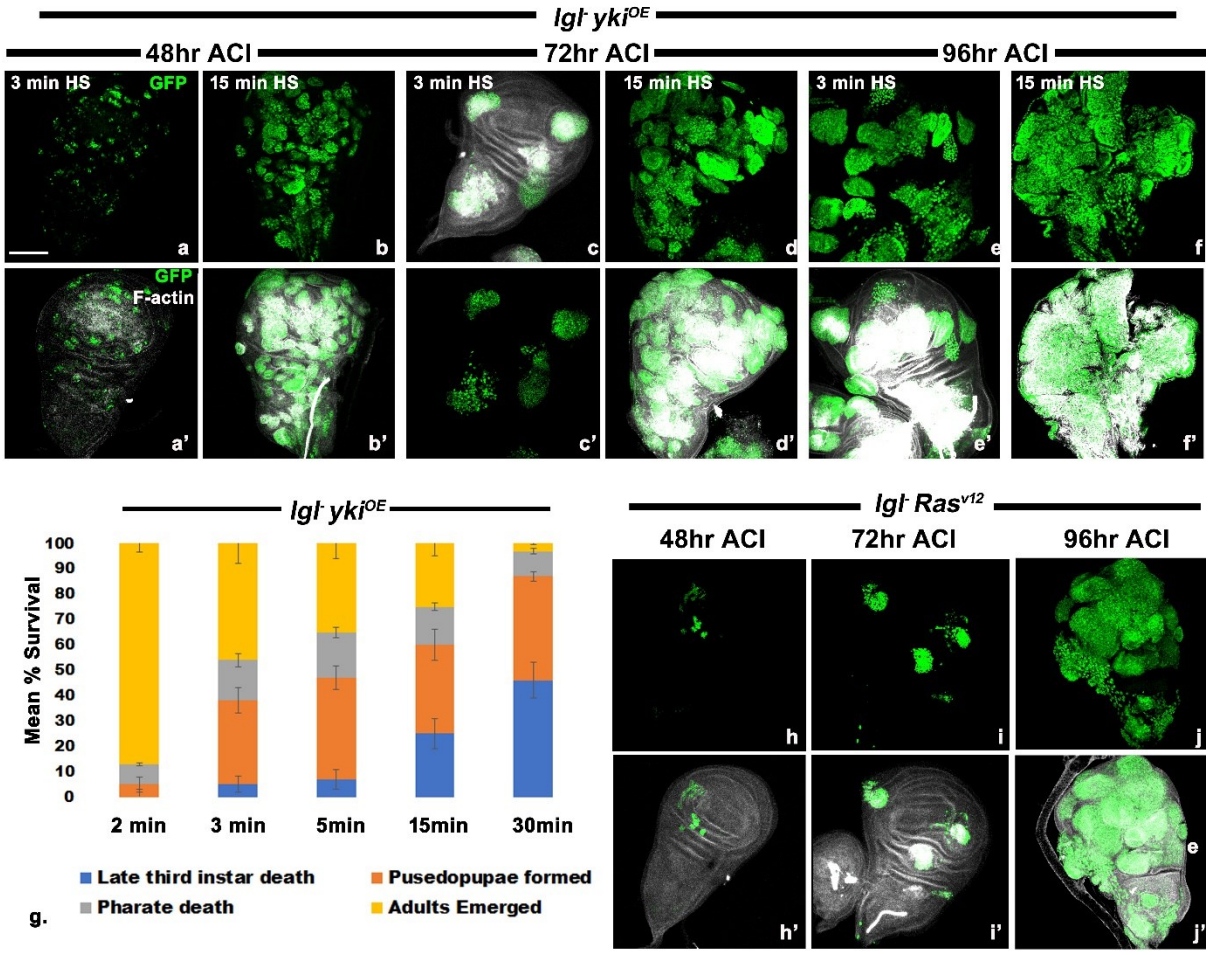

Fig. 4. Standardization of duration of HS for induction of *lgl⁻ yki*^{OE} (a-f') and *lgl⁻ Ras*^{v12} (h-j') clones. Wing discs from 72hr old larvae exposed to 3min (**a-a' c-c'** and **e-e'**) or 15min (**b-**

b', d-d' and **f-f'**) HS; those exposed to 3min HS showed small and fewer GFP expressing (green) *lgl⁻ yki*^{OE} clones (**a-a'**) which could be traced distinctly till 72hr (**c, c'**) or 96hr (**e' e'**) of tumor growth**,** which was not possible following 15min HS treatment due to massive growth of clones (**b, b', d, d', f, f'**). **g**, Histograms of mean percentage (± S.E.) of survival till different developmental stages (**Y-axis**) of the 72hr old larvae exposed to different durations of HS to induce *lgl⁻ yki*^{OE} somatic clones (**X-axis**). (**h-j'**) Wing discs at different times ACI (noted above each column) following 5min HS to 72hr old larvae showing distinct *lgl⁻ Ras*^{v12} clones. Images in **a'-f'** and **h'-j'** show combined GFP (green) and F-actin (white) fluorescence. Scale bar in **a** denotes for 50µm and applies to **a-j'** except **g**.

Generating tumors in wing discs following down-regulation of polarity gene function with or without coincident gain of function of oncogenes using *MS1096-GAL4* driver

In agreement with earlier report (Capdevila and Guerrero 1994), the *MS10960-GAL4 (*referred to as *MS1096*) directed *UAS-GFP* reporter transgene (*MS1096>UAS-GFP*) is expressed in the presumptive wing blade region and in some parts of hinge and notum (inset in **Fig. 5a**). In addition, it was also found to express in optic lobes of brain and salivary glands during larval stages (not shown). *UAS-lgl*^{RNAi} driven by *MS1096* was used to down regulate the Lgl activity in wing discs (**Fig. 5a-a', b-b'**). Compared to wing discs from undriven *lgl*^{RNAi} (**Fig. 5a-a'**), down-regulation of *lgl* via *MS1096>UAS-lgl*^{RNAi} resulted in defects in cytoskeleton in wing disc cells as revealed by staining F-actin with Phalloidin (**Fig. 5b-b'**) but not in tumorous growth.

MS1096 driven over expression of active *Ras*^{v12} by itself promoted over-growth of wing discs with disrupted cytoskeleton (**Fig. 5 c-c'**) while co-expression of *UAS-Ras*^{v12} and *lgl*^{RNAi} (*MS1096>UAS-Ras*^{v12}*; lgl*^{RNAi}) in wing discs resulted in malignant tumorous overgrowth (**Fig. 5d-d'**). Over-expression of Yorkie in *MS1096>yki*^{OE} wing discs resulted only in distorted wing pouch region without any tumor (not shown). However, these larvae died at pupal stage. Another transgene over-expressing a mutant form of Yorkie, *yki*^{Act}*,* which produces an activated form of Yorkie and generates intestinal tumors (Known et al 2016), when driven by the *MS0196 (MS0196>yki*^{Act}) developed massively tumorous wing discs with actin-nucleation, a typical feature of cancer cells and a huge increase in size (**Fig. 5e-e'**). Similarly, *MS1096>UAS-Pvr*^{Act} wing discs also displayed massive over-growth with actin nucleation (**Fig. 5f-f'**).

Follow up of development of larvae of the above different genotypes revealed that all un-driven as well as *MS1096* driven lgl^{RNAi} larvae pupated and emerged as adults but all larvae of the other genotypes, except *MS1096>*Ras^{v12}, died before reaching the adult stage; a few pupae in the case of *MS1096>*Ras^{v12} emerged as flies. Unlike the undriven *UAS-*lgl^{RNAi} flies (Fig. 3.7 a-a''), the *MS1096>lgl-RNAi* adults showed various wing deformities (not shown).

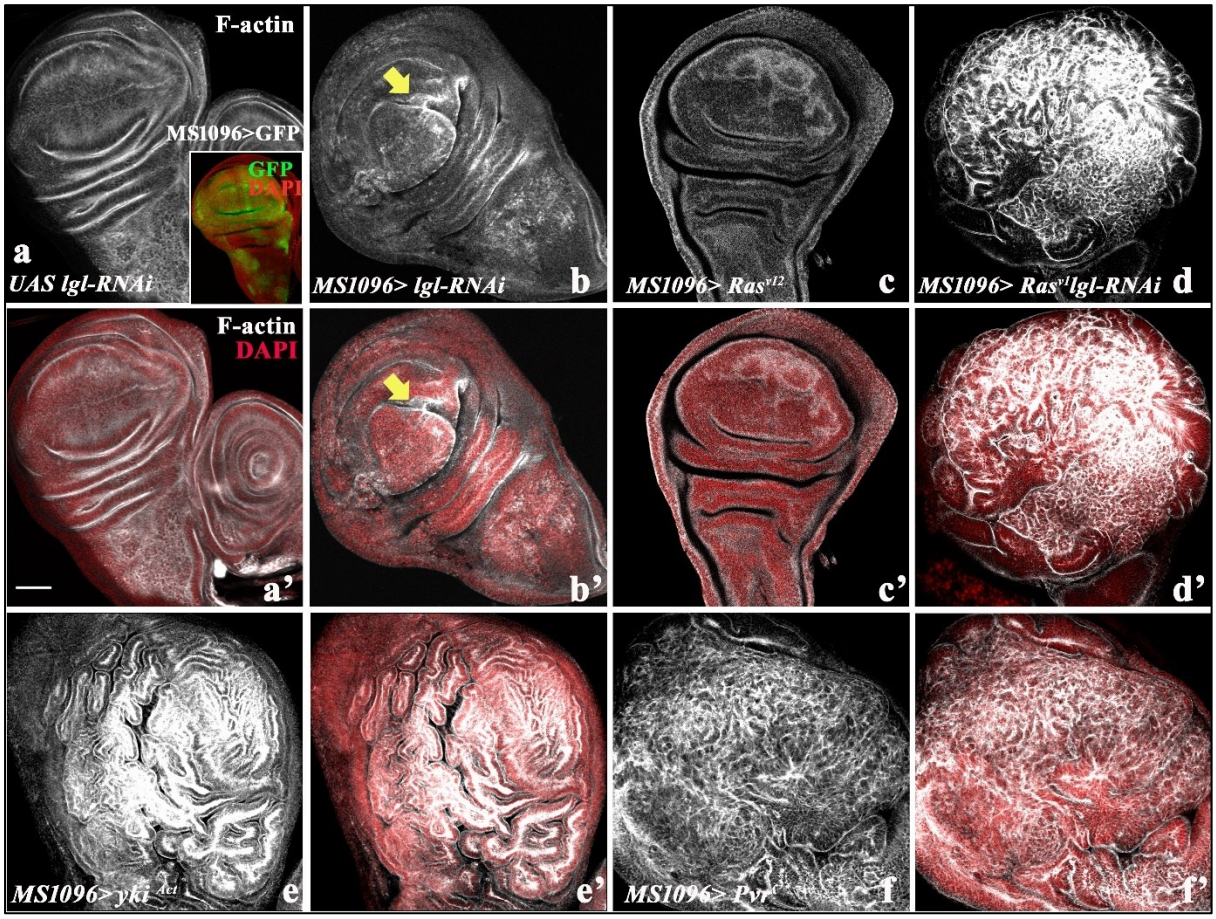

Fig. 5. Wing discs showing effects of loss of *lgl* polarity gene activity and/or gain of function of other oncogenes on tissue morphology and cytoskeleton: Compared to control (undriven lgl^{RNAi}) wing discs (**a-a'**), the *MS1096* driven loss of *lgl* transcripts in *MS1096>*lgl^{RNAi} resulted in deformed tissue organization (**b-b'**); inset in (**a**) shows expression domain of the *MS1096* driver in *MS1096>UAS-GFP* (green) wing discs. *MS1096* driven active Ras^{v12} expression affected tissue morphology without any tumorous growth (**c-c',**) but co-expression of *MS1096>*lgl^{RNAi} and Ras^{v12} resulted in aggressive tumorous growth (**d-d'**). *MS1096* driven over-expression of activated Yorkie (yki^{Act}) or Pvr (Pvr^{Act}) caused aggressive tumors in wing discs (**e-e'** and **f-f',** respectively). The genotypes are noted at lower left corner in **a-f**, which show Phalloidin-stained (white) F-actin; **(a'-f')** are images of corresponding **(a-f)** discs showing DAPI-stained nuclei (red) and Phalloidin-stained F-actin (white). Yellow arrows

in (**b-b'**) indicate the folds due to disruption in growth. Scale bar in **a'** denotes for 50µm and applies to **a-f'**.

Patterns of expression of major heat shock proteins during tumor progression in wing discs

Following the above initial characterization and standardization of induction of tumors in wing discs in different genotypes, patterns of expression of the major heat shock proteins (Hsp83, Hsp70, Hsp60 and Hsp27) in tumorous wing discs were examined. The tumors were induced either as MARCM clones for examination of the expression of the Hsps in the clones at different time points ACI compared to that in the normal surrounding cells or as *Act-Gal4* or *MS1096* induced wing-blade tumors. At least 20-30 imaginal discs of each of the examined genotype at different time points were examined for immunostaining with antibodies that detect the given Hsp. The discs were also co-stained with Phalloidin (to detect F-actin) and DAPI (DNA).

Hsp27 expression in ***lgl⁻ yki^{OE}*** **and** ***lgl⁻ Ras^{v12}*** **clones**

Enhanced levels of Hsp27 were seen in *lgl⁻ yki^{OE}* neoplastic clonal cells at 48hr ACI by 3min HS to 72hr (AEL) larvae, particularly in cells which were present at the periphery creating a ring like structure (**Fig. 6a-a''**) which further increased at later stages (**Fig. 6b-c''**). The *lgl⁻ Ras^{v12}* neoplastic cells exhibited a similar pattern of Hsp27 expression during their progression (**Fig. 6d-d'').**

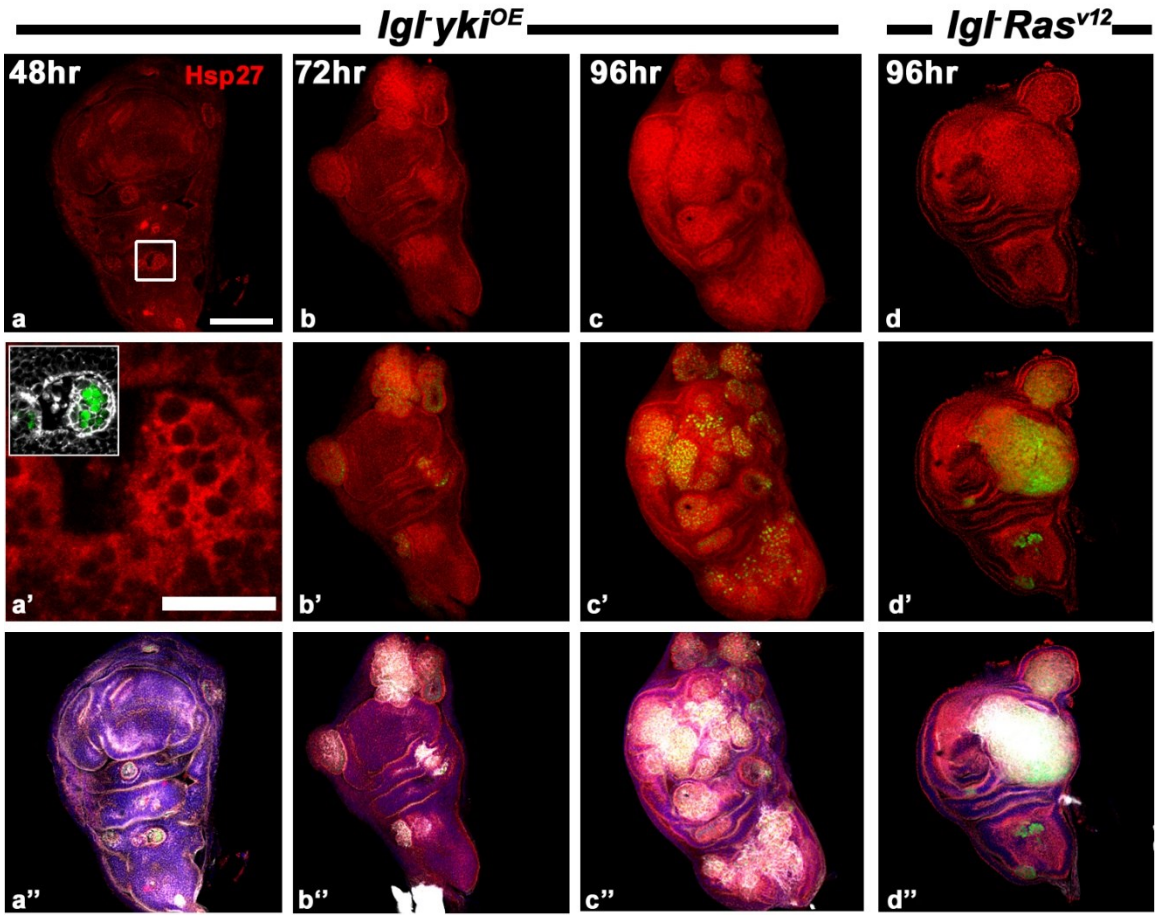

Fig. 6. Neoplastic cells over express Hsp27 since the beginning of their development till late stages of progression. Tumrous clones of *lgl⁻ yki^OE* in wing imaginal discs showing over-expression of Hsp27 (red) at 48hr ACI (**a-a''**); (**a'**) shows a single *lgl⁻ yki^OE* GFP (green) positive clone (boxed in **a** and also shown in inset in **a'**) at higher magniciation to show elevated expression of Hsp27 (**red**). (**b-c''**) *lgl⁻ yki^OE* GFP positive clones (**b'-c'**) show consistent over-expression of Hsp27 at 72hr ACI (**b-b''**) and 96hr ACI (**c-c''**). (**d-d''**) *lgl⁻ Ras^v12* clones showing enhanced Hsp27 at 96hr ACI. (**a'', b'', c'', d''**) show combined Hsp60 (red), GFP (green), DAPI (blue) and Phalloidin (white) fluorescence. Scale bar in **a** represents 50µm and applies to all except **a'**; the scale bar in **a'** scale indicates 20µm.

Hsp60 expression in ***lgl⁻ yki^OE*** **and** ***lgl⁻ Ras^v12*** **clones and** ***Act>lgl^RNAi*** **and** ***MS1096> yki^OE*** **wing discs**

Levels of Hsp60 in *lgl⁻ yki^OE* neoplastic cells were enhanced at 48hr ACI (**Fig. 7a-a''**), which further increased at later stages (**Fig. 7b-c''**). The *lgl⁻ Ras^v12 MARCM* clonal neoplastic cells exhibited a similar pattern of Hsp60 expression during their initial and later stages of growth

(**Fig. 7d-d”).** The *Act>lglRNAi* and *MS1096>yki*^{Act} tumorous discs also uniformly expressed enhanced levels of Hsp60 during tumor growth (**Fig. 3.10 e-f’**).

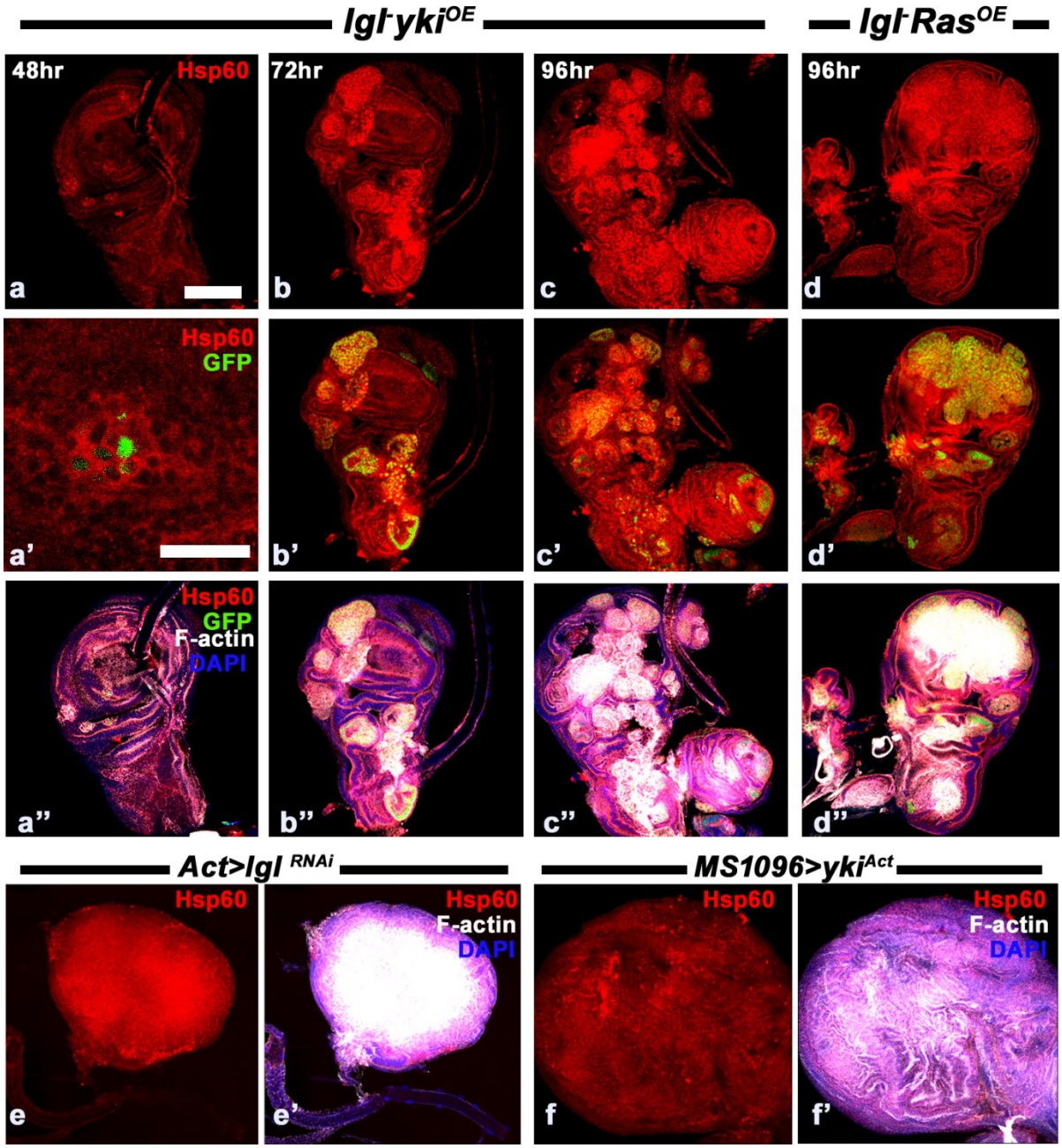

Fig. 7. Neoplastic cells over express Hsp60 since the beginning of their induction till late stages of progression. (**a-a’’**) GFP (green) positive *lgl*$^{-}$ *yki*^{OE} clones with over-expression of Hsp60 (**red**) at 48hr ACI; (**a’**) shows magnified image of a single clone from the disc in **a**; (**b-c”**) show elevated Hsp60 (red) in all GFP positive (green) *lgl*$^{-}$ *yki*^{OE} clones clones at 72hr (**b-b”**) and 96hr (**c-c”**) ACI; (**d-d’’**) *lgl*$^{-}$ *Ras*^{v12} clones show enhanced Hsp60 at 96hr ACI. The **b’-d**’ show Hsp60 and GFP fluorescence while **a”-d**” show Hsp60 (red), GFP (green) and Phalloidin (white) fluorescence. *Act>lglRNAi* (**e-e’)**

and *MS1096>yki*^{Act} (**f-f'**) tumrous wing discs show elevated Hsp60 protein (**red**) throughout the disc area; **e'** and **f'** show combined Hsp60 (red), DAPI (blue) and F-actin staining (white). Scale bar in **a** denotes 50µm and applies to all panels, except **a'**; the scale bar in **a'** denotes 20µm.

Hsc70 and Hsp70 expression *lgl*$^{-}$ *yki*^{OE} clones.

Proteins belonging to Hsp70 family have both contitutive as well as inducible expression patterns and all of them have been implicated in tumorigenesis (Arya et al 2007; Murphy 2012). In *Drosophila,* the inducible form is denoted as Hsp70 while the constitutive forms are grouped as Hsc70 (Arya et al 2007). Therefore, we looked at the expression of both classes of this family of proteins using two different antibodies in *lgl*$^{-}$ *yki*^{OE} MARCM clones. The 7Fb antibody detects only the stress inducible *Drosophila* Hsp70 while the 3.701 antibody detects both inducible as well as constitutive forms, i.e., Hsp70 as well as the various Hsc70 proteins (Velazquez and Lindquist, 1984). The difference between the staining patterns obtained with 3.701 and 7Fb can thus be ascribed to Hsc70 expression. Staining with 3.701 antibody showed increased levels of Hsc70/Hsp70 proteins at 48hr ACI (**Fig. 8a-a'**). Surprisingly, however, the 7FB antibody did not show any Hsp70 positive cell at 48hr ACI (**Fig. 8b-b'**), implying thereby that while Hsp70 is not expressed in these clones till this time, the observed increased staining with the 3.701 antibody at 48hr ACI is due to enhanced levels of the various Hsc70 proteins in *lgl*$^{-}$ *yki*^{OE} clones since their early stages. Interestingly, while the 3.701 antibody showed further enhanced staining across the full clone area at 72hr ACI, more so at the clone periphery (**Fig. 8c-c'**), the 7FB antibody staining pattern was entirely different. In a majority (68) of discs at 72hr ACI, only a few of the *lgl*$^{-}$ *yki*^{OE} clone cells were strongly 7FB positive (**Fig. 8d-e'**, marked with yellow arrows) with negligible staining of rest of the clone area. In a few other discs/clones, the entire clonal area expressed Hsp70 at a low level with a few cells showing a much higher Hsp70 staining (**Fig. 8d-d'**, marked with white arrows).

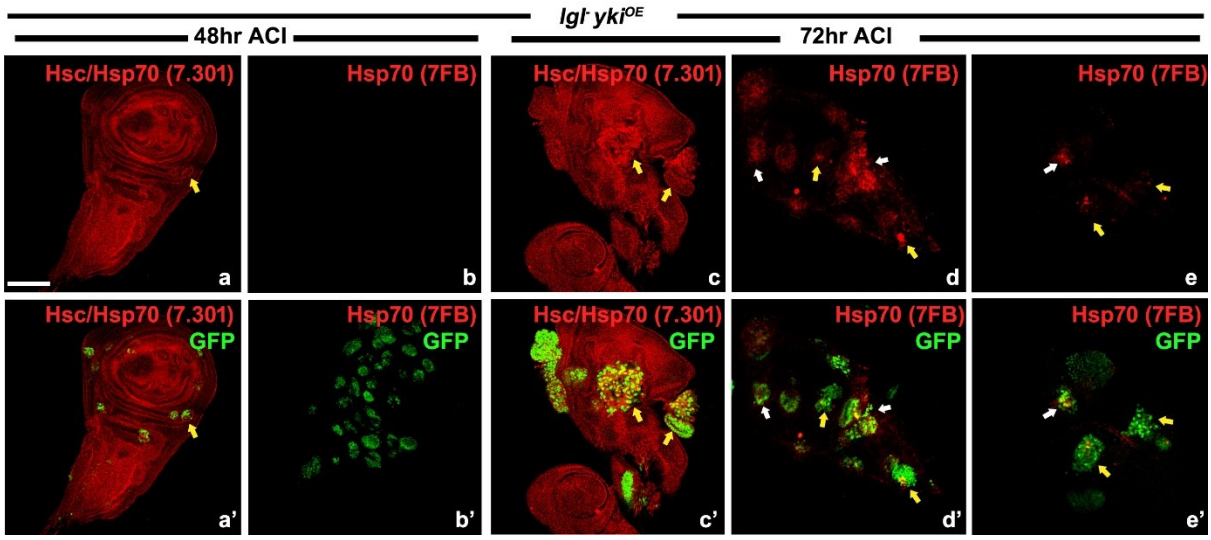

Fig. 8. Neoplastic cells (*lgl⁻ yki^OE*) over express Hsc70 since the early stages of their development, but Hsp70 is expressed only in a few *lgl⁻ yki^OE* cells at later stages. (**a-a'**) Wing imaginal disc with GFP positive *lgl⁻ yki^OE* clones (green) showing over-expression of Hsc70/Hsp70 (red) at 48hr ACI. (**b-b'**) Wing imaginal disc with GFP positive *lgl⁻ yki^OE* clones (green) without any staining for 7Fb positive Hsp70 (red) staining at 48hr ACI. **c-c'** Enhanced expression of Hsc-70/Hsp70 (red) in the entire area of tumorous clones (GFP, green) at 72hr ACI. **d-e'** Two patterns of 7Fb positive Hsp70 (red) staining in *lgl⁻ yki^OE* clones (green) at 72hr ACI: example in **d-d'** shows weak Hsp70 staining across most of the GFP-positive (green) clones (white arrows) but with a few cells in each are more intensely labelled (yellow arrows); the more common pattern illustrated in **e-e'** shows Hsp70 (red) expression only in a few of the GFP-positive *lgl⁻ yki^OE* cells. **a'-e'** show combined red and green fluorescence patterns of the discs in **a-e**, respectively. Scale bar in **a** denotes 50µm and applies to **a-e'**.

Hsp83 expression in *lgl⁻ yki^OE* clones and in tumorous wing blades

Hsp83 is the *Drosophila* homologue of mammalian Hsp90, which is a key regulator in maintaining proteostasis under both physiological and stress conditions in eukaryotic cells. The HSP90 has become a promising drug target for several diseases including cancer and several proteinopathies (Barrott and Haystead 2013, Schopf et al 2017). We examined the spatial and temporal expression of Hsp83 in different tumor backgrounds (**Fig. 9**). Enhanced levels of Hsp83 in the clonal *lgl⁻ yki^OE* neoplastic cells were observed as early as 48hr ACI, with markedly enhanced levels in cells at the periphery of each clone, creating a ring like appearance (**Fig. 9a-a''**); the Hsp70 rich regions also showed higher F-actin staining. Hsp83

expression became uniformly high all through the clonal area at 72hr and 96hr ACI (**Fig. 9b-c''**). The *lgl*$^{-}$ *Ras*^{v12} neoplastic clones also exhibited a similar pattern of Hsp83 expression during their progression (expression at 96hr ACI is shown in **Fig. 9d-d''**). The levels of Hsp83 appeared to correlate with the extent of F-actin accumulation in the clones, which increased with sizes of clones at later hr ACI (**Fig. 9**) In addition to the clonal cells, we also examined Hsp83 levels in wing discs from *Act>lglRNAi* or *MS1096>yki*^{act} larvae. Interestingly, these ubiquitously tumorous discs also showed enhanced levels of Hsp83 and F-actin all through the disc (**Fig. 9e-f'**).

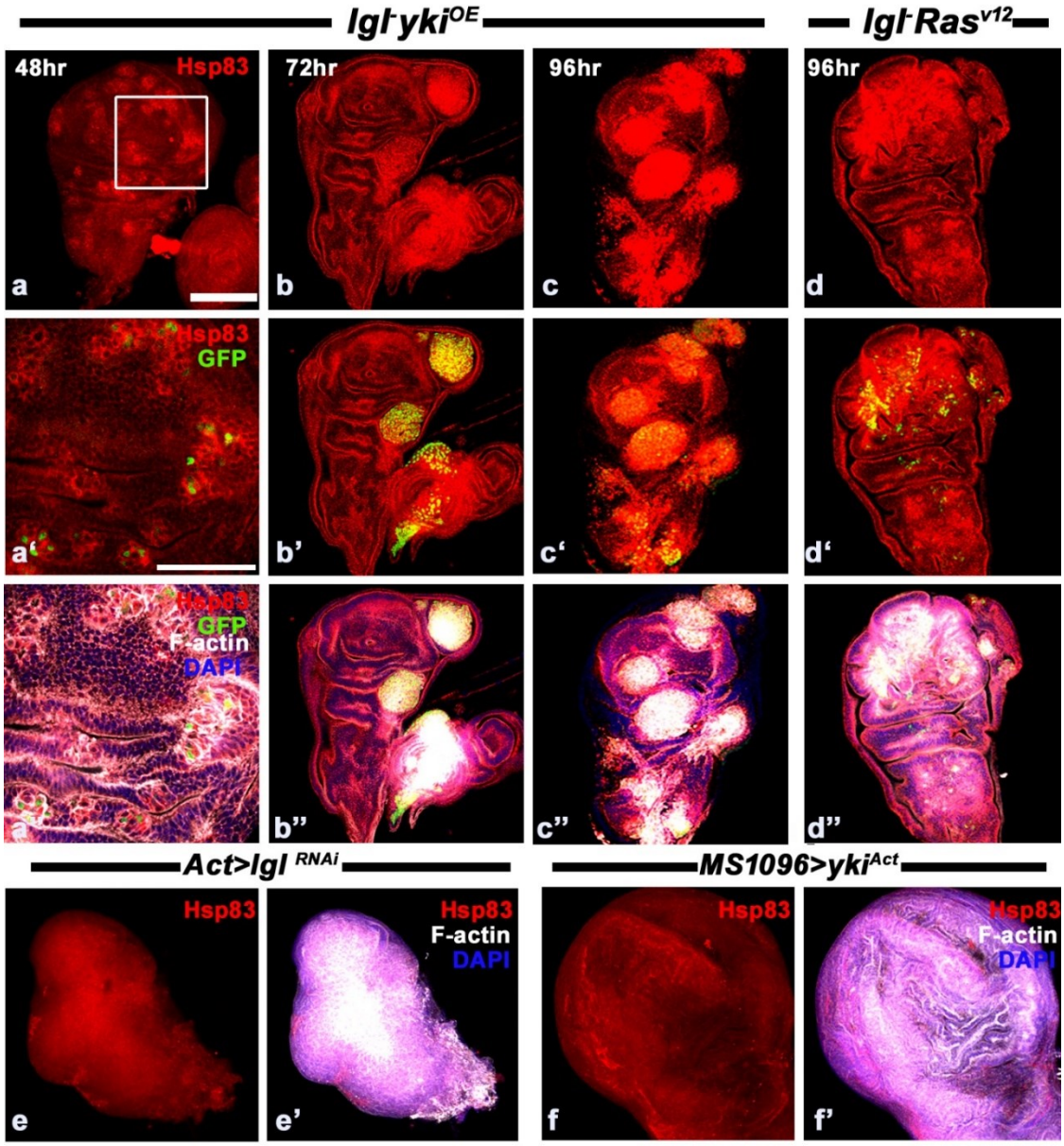

Fig. 3.12. Neoplastic cells over express Hsp83 since the beginning of their development till late stages. (a-c''): confocal optical sections showing Hsp83 (red) over-expression in *lgl*$^{-}$

yki^{OE} GFP (Green) positive clones at 48hr (**a-a"**), 72hr (**b-b"**) and 96hr (**c-c"**) ACI; **d-d''** *lgl*$^{-}$ *Ras*^{v12} tumors showing enhanced Hsp83 (red) at 96hr ACI. **a-d** show Hsp83 staining, **a'-d'** show Hsp83 and GFP expression while **a"-d"** show Hsp83 and F-actin (white) staining, respectively. (**e-f')** *Act>lglRNAi* (**e-e'**) or *MS1096>yki*^{act} (**f-f'**) tumorous wing discs showing elevated Hsp83 (red); **e'**. and **f'** show F-actin (white) and DAPI counterstaining. Scale bar in **a** denotes for 50µm and applies to **b-f'**.

Discussion

Drosophila is a well-established model for studying tumor progression, especially because the signaling pathways controlling tumor progression are largely conserved between *Drosophila* and humans (Ugur et al 2016; Mirzoyan et al 2019; Kanda and Igaki 2020). The availability of sophisticated targeting techniques like the *GAL4/UAS* binary system for conditional expression and the *FLP-FRT*- MARCM clonal analysis are some of the unique advantages offered by the fly system as they permit up- or down-regulation of the desired gene/s in specific tissues or groups of cells at defined time of development. The presence of mutant cells juxtaposed with wild-type cells in the somatic clone carrying mosaic discs also allows study of molecular basis of the tumor microenvironment required for invasion and metastasis (Miles 2011; Ohsawa 2019; Kanda and Igaki 2020).

A study of the temporal and spatial expression of Hsps during initial stages of tumor growth required standardization of the genotypes and optimal treatment conditions for induction of somatic clones. The first part of this study describes the pilot experiments undertaken to establish optimal conditions for subsequent analyses.

The *MARCM* as well as *GAL4-UAS* systems were used to generate tumors. The *MS1096-GAL4* driver provided the advantage of inducing tumors in larval wing discs by expressing the GAL4 under an endogenous promoter, because of which the induced tumors showed less variation in their progression properties. As expected, different genetic backgrounds used for generating tumorous wing discs had their distinct features. While transgenes over-expressing active Yki or Pvr under the *MS1096* driver could by themselves mediate tumor growth, down regulation of *lgl* transcripts through RNAi or over-expression of active Ras by the same driver appeared insufficient to promote a malignant tumorous growth. In agreement with earlier reports (Menendez et al 2010; Daniel 2018; Ohsawa 2019; Kanda and Igaki 2020), *MS1096* driven co-expression of *lgl-RNAi* and active Ras generated tumorous wing discs.

A limitation of the *MS1096* or *Act-GAL4* driven induction of tumors is that the target genes start expressing from early stages of development and thus do not permit precise tracking of the spatial and temporal events associated with the early stages of tumor induction and growth. The induction of tumorous somatic clones in the MARCM approach through HS induced production of the FLP-recombinase provided a convenient system for a precise temporal monitoring of the tumor growth in terms of hours after heat shock (ACI), since the induced *FLP* led somatic crossing over at the FRT sites and thus to generation of clones within a defined window. In addition, the mosaic discs permit studies on interaction between wild type cells and the clonal tumor cells, which is not possible in the *MS1096 or Act-GAL4* driven induction of tumors. Therefore, considering the specific advantages offered by each of these two approaches, the *Gal4-UAS* as well as the *MARCM* systems have been used in the present study.

Generally a 30min or 1hr HS is applied for generation of MARCM somatic clones (Lee and Luo 1999; Khan et al 2016). In the present study it was found that while a 30min HS produced analyzable lgl^{-} clones, a similar HS treatment in case of lgl^{-} yki^{OE} generated too many clones, which outnumbered wild type cells and resulted in gigantic discs filled with tumor cells. Therefore, HS duration and the developmental stage for application of HS were standardized with a view to generate discrete clones that could be tracked for longer duration. Accordingly, we found that a shorter pulse (3 or 5 min) of heat shock to 72hr old (after egg laying) generates discrete clones that can be examined for longer periods after the induction. These pilot studies also confirmed the varying propensities of progression of the lgl^{-} clones in different regions of the wing imaginal discs in relation to their genetic background. Khan et al (2016) reported that loss of Lgl in the wing primordium (notum) induced neoplasia in its proximal domain while lgl^{-} clones in the Vg expressing distal wing epithelium (wing pouch) were eliminated by cell death, transcriptional alteration targeting the cell death pathway resulted in generation of neoplasia. As expected, lgl^{-} yki^{OE}, lgl^{-} Ras^{v12} and lgl^{-} N^{ICD} clones had different growth rates and were also restricted to different compartments of wing discs. We also found (data not presented) that the lgl^{-} yki^{OE} clones and lgl^{-} N^{ICD} clones flourished throughout the disc while lgl^{-} Ras^{v12} clones were restricted to the wing pouch region. Interestingly despite the slower growth of lgl^{-} Ras^{v12} and $lgl^{-}N^{ICD}$ genotype in comparison to lgl^{-} yki^{OE}, these larvae showed greater lethality than seen in lgl^{-} yki^{OE} clone-carrying larvae. This indicates that despite the slower growth, these tumorous clones have greater systemic effect.

Hsps are the major components of a universal and rapid response to cellular stresses for restoring homeostasis. Consequently, heat shock proteins assist in recovery from stress either by repairing damaged proteins (protein refolding) or by degrading them and thus promoting cell survival (Morimoto et al 1992; Arya et al 2007). Cells or tissues from a wide range of tumors have been shown to express atypical levels of one or more Hsps and, due to their importance in maintaining the stability, integrity, conformation and function of key oncogenic proteins have gained interest as promising anticancer drug targets (Calderwood et al 2016; Bastola et al 2018; Aswad and Liua 2021). Hsps also play fundamental roles in processes of signal transduction, cell cycle progression and apoptosis, cell proliferation and survival, as well as other features of malignant cells, such as invasion, metastasis and tumor angiogenesis via client proteins (Calderwood 2018).

In this study, *Drosophila* tumors with lgl^{-} yki^{OE} and lgl^{-} Ras^{v12} neoplastic clonal cells exhibited increase in the expression of Hsp83, Hsc70, Hsp60 and Hsp27 since the early stage of clonal progression. With further progression, all these proteins showed elevation in nearly all of the tumorous clonal cells. When tumors were induced all through the imaginal discs using *Act-Gal4* or *MS1096* driver to express *lgl-RNAi* or Yki^{OE} transgene, the Hsp levels were found to be uniformly enhanced all through the disc. Earlier studies in mammalian cancers have also reported enhanced levels of different Hsps (Workman et al 2004; Calderwood 2018). Our other studies (Gunjan Singh and Lakhotia, in preparation) using the present model for inducing tumors show that perturbations in levels of these different proteins promotes or retards the clonal growth by modulating apoptosis and/or apoptosis induced proliferation (Diwanji and Bergmann 2019).

A very significant finding of the present study, which was possible because of the unique design of clone induction and temporal tracking of their development, was the spatio-temporally restricted pattern of expression of Hsp70 in lgl^{-} yki^{OE} clonal cells when they acquire neoplastic property. This pattern is completely different from the globally enhanced expression of the other major Hsps from the early stages of tumor growth Such a patterns of Hsp70 expression in tumors has not been reported. Significance and functional consequences of the unique and intriguing pattern of Hs70 expresion in the tumorous clones reported here is being examined.

Acknowledgements. We acknowledge the Department of Biotechnology (Govt.of India) for the initial support for this project (no. BT/PR14716/BRB/10/876/2010) and the Science &

Engineering Research Board (Govt. of India) for currently supporting SCL. Gunjan Singh was supported by the University Grants Commission (New Delhi). We thank Prof. Pradip Sinha (IIT, Kanpur, India) and the Bloomington Drosophila Stock Center for different fly stocks. We also thank Prof. M. Evgen'ev (Russia) and Prof. Robert Tanguay (Canada) for providing Hsp70 and Hsp83 antibodies, respectively.

References

Agrawal, N., Kango, M., Mishra, A. and Sinha, P. (1995b). Neoplastic transformation and aberrant cell-cell interactions in genetic mosaics of *lethal(2) giant larvae (lgl*), a tumor suppressor gene of *Drosophila*. Developmental Biology 172: 218-228.

Arya R., Mallik M. and Lakhotia S. C. 2007 Heat shock genes - integrating cell survival and death. *J Biosci* **32,** 595-610.

Aswad, A., and Liu, T. 2021. Targeting heat shock protein 90 for anti-cancer drug development. *Advances in Cancer Research*, 152, 179-204.

Barrott J. J. and Haystead T. A. 2013 Hsp90, an unlikely ally in the war on cancer. *Febs j* **280,** 1381-96.

Bastola, P., Oien, D. B., Cooley, M., anf Chien, J. 2018. Emerging cancer therapeutic targets in protein homeostasis. *The AAPS Journal*, 20, 1-15.

Betschinger J., Mechtler K. and Knoblich J. A. 2003 The Par complex directs asymmetric cell division by phosphorylating the cytoskeletal protein Lgl. *Nature* 422, 326-30.

Calderwood, S. K. (2018). Heat shock proteins and cancer: intracellular chaperones or extracellular signalling ligands?. *Philosophical Transactions of the Royal Society B: Biological Sciences*, 373, 20160524.

Calderwood S. K. and Gong J. 2016 Heat shock proteins promote cancer: It's a protection racket. *Trends Biochem Sci* 41, 311-323.

Calderwood S. K., Khaleque M. A., Sawyer D. B. and Ciocca D. R. 2006 Heat shock proteins in cancer: chaperones of tumorigenesis. *Trends Biochem Sci* 31, 164-72.

Calderwood S. K. and Murshid A. 2017 molecular chaperone accumulation in cancer and decrease in Alzheimer's disease: The potential roles of HSF1. *Front Neurosci* 11, 192.

Capdevila J., Estrada M. P., Sánchez-Herrero E. and Guerrero I. 1994 The Drosophila segment polarity gene patched interacts with decapentaplegic in wing development. *Embo j* 13, 71-82.

Daniel S. G., Russ A. D., Guthridge K. M., Raina A. I., Estes P. S., Parsons L. M.*, et al.* 2018 miR-9a mediates the role of lethal giant larvae as an epithelial growth inhibitor in Drosophila. *Biol Open* **7**.

Diwanji N. and Bergmann A. 2019 Two sides of the same coin - compensatory proliferation in regeneration and cancer. *Adv Exp Med Biol* 1167, 65-85.

Drubin D. G. and Nelson W. J. 1996 Origins of cell polarity. *Cell* 84, 335-44.

Fristom D. and Fristom J. W. 1975 The mechanism of evagination of imaginal discs of Drosophila melanogaster. 1. General considerations. *Dev Biol* 43, 1-23.

Fristrom J. W. 1970 The developmental biology of Drosophila. *Annu Rev Genet* 4, 325-46.

Froldi F., Ziosi M., Tomba G., Parisi F., Garoia F., Pession A.*, et al.* 2008 Drosophila lethal giant larvae neoplastic mutant as a genetic tool for cancer modeling. *Curr Genomics* 9, 147-54.

Gateff E. and Schneiderman H. A. 1974 Developmental capacities of benign and malignant neoplasms ofDrosophila. *Wilhelm Roux Arch Entwickl Mech Org* 176, 23-65.

Hanahan D. and Weinberg R. A. 2011 Hallmarks of cancer: the next generation. *Cell* 144, 646-74.

Heino T. I., Kärpänen T., Wahlström G., Pulkkinen M., Eriksson U., Alitalo K.*, et al.* 2001 The Drosophila VEGF receptor homolog is expressed in hemocytes. *Mech Dev* **109,** 69-77.

Huang, J., S. Wu, J. Barrera, K. Matthews and D. Pan (2005). The hippo signaling pathway coordinately regulates cell proliferation and apoptosis by inactivating yorkie, the Drosophila homolog of YAP. Cell 122: 421-434

Hutterer A., Betschinger J., Petronczki M. and Knoblich J. A. 2004 Sequential roles of Cdc42, Par-6, aPKC, and Lgl in the establishment of epithelial polarity during Drosophila embryogenesis. *Dev Cell* 6, 845-54.

Kanda H. and Igaki T. 2020 Mechanism of tumor-suppressive cell competition in flies. *Cancer Sci* **111,** 3409-3415.

Khan S. J., Bajpai A., Alam M. A., Gupta R. P., Harsh S., Pandey R. K.*, et al.* 2013 Epithelial neoplasia in Drosophila entails switch to primitive cell states. *Proc Natl Acad Sci U S A* **110,** E2163-72.

Lang B. J., Guerrero-Giménez M. E., Prince T. L., Ackerman A., Bonorino C. and Calderwood S. K. 2019 Heat shock proteins are essential components in transformation and tumor progression: Cancer cell intrinsic pathways and beyond. *Int J Mol Sci* 20. 4507*; doi:10.3390/ijms20184507*

Lee T. and Luo L. 1999 Mosaic analysis with a repressible cell marker for studies of gene function in neuronal morphogenesis. *Neuron* 22, 451-61.

Lee T. and Luo L. 2001 Mosaic analysis with a repressible cell marker (MARCM) for Drosophila neural development. *Trends Neurosci* 24, 251-4.

Morata, G. and Ripoll, P. (1975). Minutes: mutants of *Drosophila* autonomously affecting cell division rate. *Developmental Biology* 42,211-221

Mechler B. M., McGinnis W. and Gehring W. J. 1985 Molecular cloning of lethal(2)giant larvae, a recessive oncogene of Drosophila melanogaster. *Embo j* 4, 1551-7.

Menéndez, J., Pérez-Garijo, A., Calleja, M., and Morata, G. (2010) A tumor-suppressing mechanism in *Drosophila* involving cell competition and the Hippo pathway. *Proceedings of National Academy of Sciences USA*, 107 (33) 14651-14656

Mirzoyan Z., Sollazzo M., Allocca M., Valenza A. M., Grifoni D. and Bellosta P. 2019 Drosophila melanogaster: A model organism to study cancer. *Front Genet* 10, 51.

Murphy, M. E. (2013). The HSP70 family and cancer. *Carcinogenesis* 34, 1181-1188.

Ohsawa S. 2019 Elimination of oncogenic cells that regulate epithelial homeostasis in Drosophila. *Dev Growth Differ* **61,** 337-342.

Parsons L. M., Portela M., Grzeschik N. A. and Richardson H. E. 2014 Lgl regulates Notch signaling via endocytosis, independently of the apical aPKC-Par6-Baz polarity complex. *Curr Biol* 24, 2073-2084.

Román-Fernández A. and Bryant D. M. 2016 Complex polarity: building multicellular tissues through apical membrane traffic. *Traffic* 17, 1244-1261.

Schopf F. H., Biebl M. M. and Buchner J. 2017 The HSP90 chaperone machinery. *Nature Reviews Molecular Cell Biology* **18,** 345-360.

Shibuya M. 2011 Vascular endothelial growth factor (VEGF) and its receptor (VEGFR) signaling in angiogenesis: a crucial target for anti- and pro-angiogenic therapies. *Genes Cancer* **2,** 1097-105.

Ugur B., Chen K. and Bellen H. J. 2016 Drosophila tools and assays for the study of human diseases. *Dis Model Mech* **9,** 235-44.

Velazquez J. M. and Lindquist S. 1984 hsp70: nuclear concentration during environmental stress and cytoplasmic storage during recovery. *Cell* 36, 655-62.

Workman P., Burrows F., Neckers L. and Rosen N. 2007 Drugging the cancer chaperone HSP90: combinatorial therapeutic exploitation of oncogene addiction and tumor stress. *Ann N Y Acad Sci* **1113,** 202-16.